JOURNAL OF SOLID STATE CHEMISTRY 91, 32–40 (1991)

Some New Perovskite-Related Compounds in the $BaO–Tl_2O_3$ System

W. ZHOU, R. S. LIU, AND P. P. EDWARDS

Interdisciplinary Research Centre in Superconductivity, University of Cambridge, Madingley Road, Cambridge, CB3 0HE, United Kingdom

Received August 8, 1990; in revised form October 15, 1990

Two new perovskite-related phases in the Tl_2O_3–BaO system have been synthesized and investigated by X-ray powder diffraction and high resolution electron microscopy. A solid solution phase exists with the compositions between $BaTl_2O_4$ and $Ba_4Tl_{10}O_{19}$. The typical composition, $Ba_6Tl_{14}O_{27}$, has an orthorhombic unit cell with $a = 17.724$, $b = 6.890$, and $c = 10.235$ Å. The compound $Ba_2Tl_{10}O_{17}$ has a $1 \times 3.5 \times 1$ superstructure derived from the $Ba_6Tl_{14}O_{27}$ phase, being also orthorhombic with unit cell dimensions of $a = 17.676$, $b = 24.167$, and $c = 10.110$ Å. The relationships between both these new structures, the recently discovered $Ba_4Tl_6O_{13}$ and the perovskite-like basic structures, are discussed.

Introduction

Partly because the synthesis of Tl-containing compounds is relatively difficult and most of these materials are poisonous, thallium chemistry was not an active field until the discovery of new high Tc superconductors $Tl_mBa_2Ca_nCu_{n+1}O_x$ ($m = 1, 2$; $n = 0, 1, 2, 3$). At present, the structures of Tl-containing ternary oxides, e.g., Tl–Cu–O, Tl–Ba–O, etc., are perhaps less well characterized than the more complicated superconducting phases.

Tl_2O_3 exists in a body-centered cubic structure of C rare-earth sesquioxide type with $a = 10.54$ Å (*1*), which is normally regarded as a defect fluorite-like structure and has quite low electrical resistivity (ca. 10^{-4} Ω cm at room temperature) (*1b*). Such a structure might be assumed to have the ability to incorporate many metal pentoxides or trioxides, forming various fluorite-related solid solutions as found, for example, in the case of Bi_2O_3 (*2, 3*). Ba oxides are, however, not good candidates for stabilizing the fluorite structure of δ-Bi_2O_3. Alternatively, perovskite structure can be formed; e.g., $BaBiO_3$.

In a previous report, the Tl_2O_3–CuO system was investigated. No binary compounds were observed; rather, a Tl_2O_3-related solid solution, $Tl_{2-x}Cu_xO_3$ (*4*), forms for the homogeneity range $0 < x < 0.12$. It might be that the relatively small size of Cu^{2+} (ca., 0.72 Å of radius) makes it possible to replace Tl^{3+} (0.95 Å) without any major structural changes in Tl_2O_3. On the other hand, Ba^{2+} (1.34 Å) is almost certainly too large to substitute directly for Tl^{3+} in this lattice. Instead, a perovskite structure is possible with the lattice tolerance factor, $t = (R_A + R_O)/[\sqrt{2}(R_B + R_C)]$, being about 0.83, where R_A, R_B, and R_O are ionic radii of Ba^{2+}, Tl^{3+}, and O^{2-} (1.32 Å). In the Tl_2O_3–BaO system, $Ba_2Tl_2O_5$ seems to be the only compound whose structure is rela-

0022-4596/91 $3.00

tively well understood. It was proposed to be $Ca_2Fe_2O_5$-like (*5*), having an orthorhombic unit cell with a = 6.264, b = 17.258, and c = 6.05 Å (*6*). The structure was also regarded to be perovskite-related as reported recently. (*7*) However, in our own previous work, (*8*) $Ba_2Tl_2O_5$ has been reinvestigated and the unit cell has been redetermined to be monoclinic with a = 5.836, b = 6.226, c = 17.342 Å and γ = 91.34°, although we still believe that the structure of $Ba_2Tl_2O_5$ is related to a distorted perovskite sublattice. We have also reported the discovery of a new compound, $Ba_4Tl_6O_{13}$, which has an orthorhombic unit cell with a = 5.748, b = 7.221, and c = 9.361 Å. It is very difficult to prepare monophasic specimens for both of these compounds. Furthermore, in the preparation process for $Ba_4Tl_6O_{13}$, we found some evidence of other Tl-rich phases which were unidentified at that time.

In this present work, we report the synthesis and structural studies of two new phases with the compositions of $Ba_2Tl_{10}O_{17}$ and $Ba_6Tl_{14}O_{27}$. We find that both of the two structures are strongly related to the perovskite lattice, and the previously reported $Ba_4Tl_6O_{13}$ is an intermediate phase between $Ba_2Tl_2O_5$ and these new compounds.

Experimental

Specimens were prepared by solid solid reaction of BaO_2 and Tl_2O_3 with nominal compositions of BaO_2–Tl_2O_3, $6BaO_2$–$7Tl_2O_3$, BaO_2–$2Tl_2O_3$, and $2BaO_2$–$5Tl_2O_3$. A mixture of oxides was ground in a mortar and pestle, pressed into a pellet, 10 mm in diameter and 2 mm in thickness, and wrapped in a gold foil to alleviate loss of thallium during the preparation. The pellet was then placed into a furnace in an oxygen atmosphere, where the temperature was increased from room temperature to 650°C at a rate of 10°C/min. The specimen was heated at sinter temperature (650°C) for 20 hr, following by cooling down at a rate of 5°C/min to room temperature. The specimen was reground, pressed into a disk again, and reheated at 730°C for another 20 hr, using the same temperature program of heating and cooling. Under such synthetic conditions, we expect the cation valences of Ba and Tl to be 2+ and 3+, respectively, and all possible new phases fall into the phase diagram of the BaO–Tl_2O_3 system.

The specimens were initially characterized by X-ray powder diffractometry (XRD) using a Spectrolab CPS-120 diffractometer employing Cu$K\alpha$ radiation. The homogeneity of the specimen was examined by energy dispersive X-ray spectrometry (EDS) in a Jeol EM-200CX electron microscope. Selected area electron diffraction (SAED) patterns were recorded from the same electron microscope, where a ±45° double tilt specimen stage was used, enabling us to obtain series SAED patterns from one single microcrystal through tilting of the specimen grid. High resolution electron microscopy images were recorded from another Jeol EM-200CX electron microscope, where a new type of side-entry specimen stage (C_s = 0.52 mm, C_c = 1.05 mm, with absolute information limit ca. 0.18 nm) (*9*) was used.

Electrical resistivity measurements were performed by using a standard four-point probe method. Electrical contacts to the samples were made by fine copper wires attached to the samples with a conductive silver paint. The measurement temperature was recorded with a calibrated platinum resistor located close to the sample. The resistivity measurement system was fully automated for data acquisition.

Results and Discussion

According to the EDS results, only the specimen of $2BaO$–$5Tl_2O_3$ shows an approximately single phasic state. Twenty particles were randomly chosen for examination.

Among them, 18 particles gave an average emission line ratio, Tl $L\alpha$/Ba $L\alpha$, of 6.9(7), which corresponds to a Tl/Ba cation ratio of 4.9(5), when the EDS data from the freshly prepared $Ba_2Tl_2O_5$ was used as a reference (*8*). For the specimen of $BaO–2Tl_2O_3$, 30 particles were examined. Using the same reference data, 22 particles had an average cation ratio, Tl/Ba, of 5.0(4) and the remainder showed 2.3(7). The EDS results from these two specimens indicated a new compound with a composition of $Ba_2Tl_{10}O_{17}$ in the $BaO–Tl_2O_3$ system. We noted that the impurities in the $BaO–2Tl_2O_3$ specimen could also possibly be new phases. However, the values of the cation ratios are rather variable, suggesting a solid solution state. We then tried to prepare a pure phase with a starting composition of $6BaO_2–7Tl_2O_3$. The concentration of the $Ba_2Tl_{10}O_{17}$ phase was obviously reduced in this preparation. Seventeen in twenty particles showed an average cation ratio, Tl/Ba, of 2.4(6). For the specimen of $BaO–Tl_2O_3$, 22 particles were chosen for examination. The cation ratio, Tl/Ba, fell into two groups, 2.0(1) from 12 particles and 1.5(1) from the rest. The latter corresponds to the composition for $Ba_4Tl_6O_{13}$, which has an orthorhombic unit cell with a = 5.748, b = 7.221, and c = 9.361 Å, as discussed previously (*8*). No significant differences were observed in the SAED studies from different compositions with Tl/Ba ratios from 2.5 to 2.0. Consequently, besides $Ba_2Tl_2O_5$ and $Ba_4Tl_6O_{13}$, we believe there are at least two more phases in the $BaO–Tl_2O_3$ system, one probably being a solid solution with variable compositions from $BaTl_2O_4$ to $Ba_4Tl_{10}O_{19}$ and the other being $Ba_2Tl_{10}O_{17}$, where oxygen contents are proposed by matching the Ba^{2+} and Tl^{3+} cation valences.

Powder X-ray diffractometry was used to initially characterize these two new phases. Figure 1 shows typical XRD patterns from the specimens of $Ba_2Tl_{10}O_{17}$ and $Ba_6Tl_{14}O_{27}$, respectively. It is interesting that these two

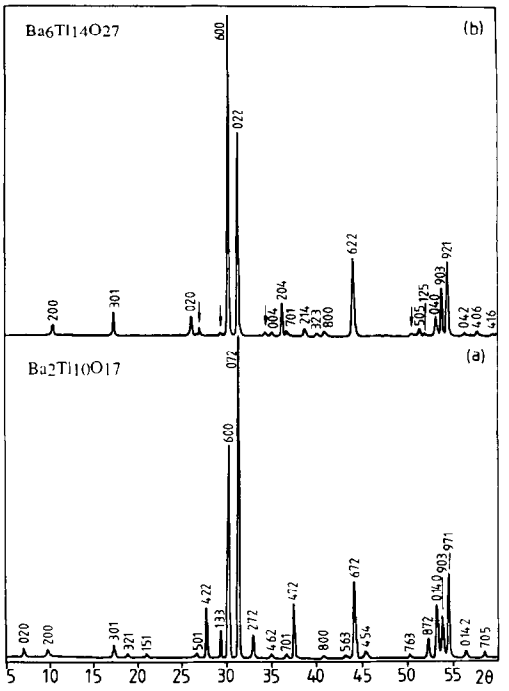

FIG. 1. XRD spectra of $Ba_2Tl_{10}O_{17}$ (a) indexed onto an orthorhombic unit cell with a = 17.676, b = 24.167, and c = 10.110 Å, and $Ba_6Tl_{14}O_{27}$ (b) indexed to an orthorhombic unit cell with a = 17.724, b = 6.890, and c = 10.235 Å. The extra lines in (b) marked by arrows are from impurity phase $Ba_2Tl_{10}O_{17}$.

phases have XRD patterns with many identical peaks, although the relative intensities of the two strongest peaks are different. To identify individual structures in a multiphasic specimen or to obtain superstructural information, SAED has proved to be a particularly powerful technique, since it can examine the structures and compositions of individual single microcrystals. Moreover, in many cases, the intensities of diffraction peaks on SAED patterns from superstructures are much stronger than those in an XRD spectrum. In the present work, we obtained the preliminary unit cell dimensions from the SAED studies. Figure 2 shows a series of SAED patterns from one microcrystal of $Ba_6Tl_{14}O_{27}$ through tilting of the specimen grid. Since we can read the

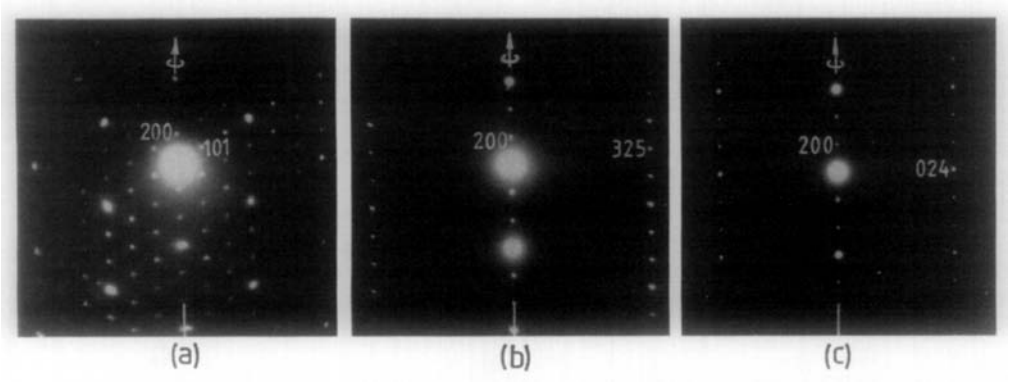

FIG. 2. SAED patterns from one single microcrystal of $Ba_6Tl_{14}O_{27}$ through tilting the specimen grid.

angles of the tilting around a certain zone axis (shown by arrows in Fig. 2) with reasonable accuracy, we can get a smallest reciprocal lattice after locating all reflection spots of these SAED patterns into a three-dimensional space. The real space unit cell for $Ba_6Tl_{14}O_{27}$ was then determined to be orthorhombic and three unit cell dimensions, a = 17.72, b = 6.89, and c = 10.24 Å, were designated. Using this unit cell, therefore, we can index all the reflection spots in SAED patterns obtained from $Ba_6Tl_{14}O_{27}$ crystals (Fig. 2). We noted the systematic absence of the diffraction spots, showing a possible body-centered symmetry in the structure ($h + k + l = 2n$). Most of the reflection lines in the XRD spectrum of $Ba_6Tl_{14}O_{27}$ (Fig. 1b) can also be indexed by using this unit cell. The remaining peaks must belong to the $Ba_2Tl_{10}O_{17}$ phase, as indicated by EDS analysis and the comparison with the XRD pattern in Fig. 1a. The unit cell parameters of $Ba_6Tl_{14}O_{27}$ were refined from the XRD spectrum to be a = 17.724, b = 6.890, and c = 10.235 Å. The body-centered nature indicated by the SAED studies might be correct in the XRD investigation if one weak peak indexed (214) in Fig. 1b is from some contaminants.

Figure 3 shows another set of SAED patterns from a single microcrystal of $Ba_2Tl_{10}O_{17}$. Using the same method described above, the unit cell calculated from these patterns is also orthorhombic with a = 17.68, b = 24.17, and c = 10.11 Å. Note that the a and c dimensions for both phases of $Ba_6Tl_{14}O_{27}$ and $Ba_2Tl_{10}O_{17}$ are very similar and the b dimension of $Ba_2Tl_{10}O_{17}$ is ca. 3.5 times the b dimension in the $Ba_6Tl_{14}O_{27}$ phase. Therefore, the $Ba_2Tl_{10}O_{17}$ phase actually is a $1 \times 3.5 \times 1$ superstructure derived from the $Ba_6Tl_{14}O_{27}$ phase. Using these unit cell parameters, the XRD pattern of $Ba_2Tl_{10}O_{17}$ (Fig. 1a) has been perfectly indexed without any observable extra peaks. The refined unit cell dimensions from XRD are thus a = 17.676, b = 24.167, and c = 10.110 Å. The symmetry of $Ba_2Tl_{10}O_{17}$ is lower than that of $Ba_6Tl_{14}O_{27}$. Both the SAED and the XRD patterns from $Ba_2Tl_{10}O_{17}$ show $h + l = 2n$ and no conditions for k rather than $h + k + l = 2n$ for $Ba_6Tl_{14}O_{27}$. Although we do not think we are able to determine the space groups at this stage, this information is certainly useful in understanding the cation arrangements in the new compounds.

As expected, the XRD pattern of $BaO-2Tl_2O_3$ is similar to that in Fig. 1b with higher intensities of $Ba_2Tl_{10}O_{17}$ peaks. The XRD pattern for $BaO-Tl_2O_3$ shows a group of impurity reflection lines of $Ba_4Tl_6O_{13}$, coexisting with the main pattern identical to Fig. 1b.

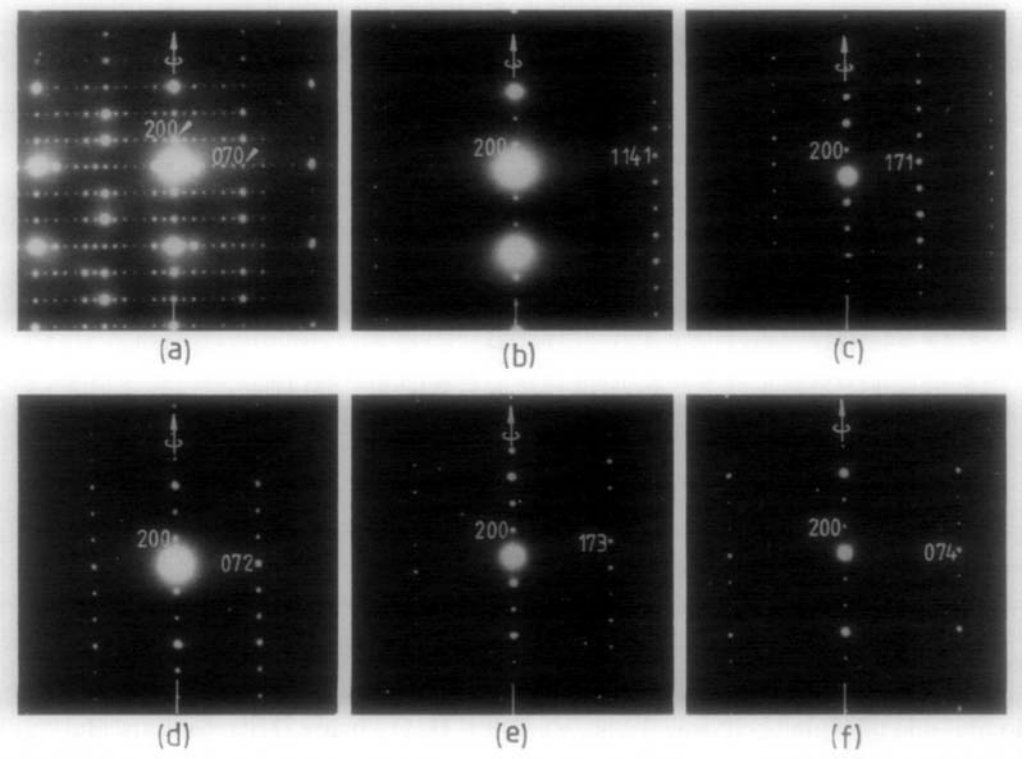

FIG. 3. SAED patterns from one single microcrystal of $Ba_2Tl_{10}O_{17}$ through tilting the specimen grid.

From the relative intensities of the diffraction spots on the SAED patterns in Fig. 2, a much more basic lattice can be determined; this is pseudocubic with $a = 4.17$ Å, from which the real structure is derived. This lattice dimension fits the perovskite structure and suggests that there might be some perovskite-like $BaTlO_{3-x}$ components in the structure. The relationship between the perovskite-like basic unit cell and the superunit cell of $Ba_6Tl_{14}O_{27}$ is:

$$\mathbf{a} = 3\mathbf{a}_b + 3\mathbf{b}_b,$$
$$\mathbf{b} = \mathbf{a}_b - \mathbf{b}_b + \mathbf{c}_b,$$
$$\mathbf{c} = \mathbf{a}_b - \mathbf{b}_b - 2\mathbf{c}_b,$$

where **a, b,** and **c** are unit cell vectors of the superstructure and $\mathbf{a}_b \approx \mathbf{b}_b \approx \mathbf{c}_b$ are perovskite-like basic unit cell vectors. Obviously, the unit cell of $Ba_2Tl_{10}O_{17}$ is also derived from the perovskite lattice by the relationship

$$\mathbf{a} = 3\mathbf{a}_b + 3\mathbf{b}_b,$$
$$\mathbf{b} = \tfrac{7}{2}\mathbf{a}_b - \tfrac{7}{2}\mathbf{b}_b + \tfrac{7}{2}\mathbf{c}_b,$$
$$\mathbf{c} = \mathbf{a}_b - \mathbf{b}_b - 2\mathbf{c}_b.$$

It is interesting to compare the unit cell parameters of $Ba_4Tl_6O_{13}$ (*8*) with those of the new compound $Ba_6Tl_{14}O_{27}$. Thus the *b* and *c* dimensions of the $Ba_4Tl_6O_{13}$ and $Ba_6Tl_{14}O_{27}$ unit cells are very close and the *a* dimension of the former is nearly one third of the latter. However, the XRD and SAED patterns from these two compounds are quite different. We therefore assume that $Ba_4Tl_6O_{13}$ is actually an intermediate phase between $Ba_2Tl_2O_5$ and $Ba_6Tl_{14}O_{27}$, both being related to perovskite and that the struc-

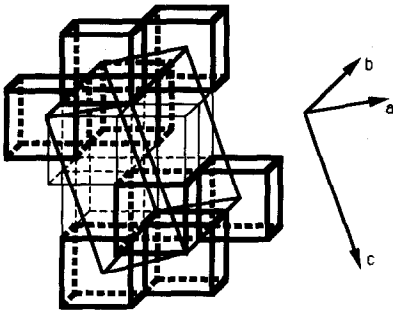

FIG. 4. A simplified model for $Ba_4Tl_6O_{13}$, showing perovskite-like blocks and the unit cell. The center sites of the bold cubes are occupied by Tl cations.

ture of $Ba_4Tl_6O_{13}$ is also derived from the perovskite lattice with the relationship

$$\mathbf{a} = \mathbf{a}_b + \mathbf{b}_b,$$
$$\mathbf{b} = \mathbf{a}_b - \mathbf{b}_b + \mathbf{c}_b,$$
$$\mathbf{c} = \mathbf{a}_b - \mathbf{b}_b - 2\mathbf{c}_b,$$

although the sublattice might be much more distorted than the other two phases. Figure 4 gives a simplified model showing the relationship between the perovskite sublattice (the cubes) and the derived superlattice of the $Ba_4Tl_6O_{13}$ phase. The plain cubes are $BaTlO_{2.5}$ with Ba in the center sites (the A sites of the perovskite lattice) and both the center sites and the corners (the B sites of the perovskite lattice) of the bold cubes are occupied by Tl cations. To distinguish Tl cations in the A sites and B sites, we use Tl^A and Tl^B. Such an ordered atomic arrangement gives rise to a $\sqrt{2} \times \sqrt{3} \times \sqrt{6}$ superlattice described above. The ideal composition of this model has a Ba/Tl cation ratio of 5 : 7. It has been noted that all $Tl^ATl^BO_3$ cubes are corner or edge sharing but not face sharing. It might be due to the manner of distortion of the Tl–O polyhedra. In this model, there are five $BaTlO_{2.5}$ cubes, two of them share faces with $Tl^ATl^BO_3$ and the other three only share edges with $Tl^ATl^BO_3$ We believe that Ba in the center sites in the latter can be further substituted by Tl cations to form even larger superlattice and solid solution materials, as observed in our experiments, i.e., $3 \times 1 \times 1$ and $3 \times 3.5 \times 1$ superstructures based on $Ba_4Tl_6O_{13}$ from $Ba_6Tl_{14}O_{27}$ and $Ba_2Tl_{10}O_{17}$, respectively. When all the B sites of the $BaTlO_{2.5}$ cubes sharing edges only with $Tl^ATl^BO_3$ in Fig. 4 are occupied by Tl, the composition becomes $Ba_2Tl_{10}O_{17}$, which is the compound observed and might be the upper compositional limit for the perovskite-related structures in the BaO–Tl_2O_3 system.

The perovskite-related natures of these new compounds were also confirmed by high resolution electron microscopy images. Figure 5 shows one of such images, taken from $Ba_2Tl_{10}O_{17}$, viewed down the $[0\bar{1}\bar{7}]$ direction of the real unit cell or the $[\bar{1}11]$ direction of the perovskite subunit cell. The pattern of the image contrast shows obviously a small pseudocubic basic lattice ($a \approx 4.1$ Å), although the real unit cell is much larger.

All of these new structures described in the present work seem to contain two kinds of blocks. One is $BaTlO_{2.5}$ and the other is $Tl^ATl^BO_3$. Since we redetermined the unit cell for $Ba_2Tl_2O_5$ (*8*), the previous result of atomic positions for this phase by X-ray diffraction refinement (*6*) might not be correct. Therefore, whether the Tl cations were in two different oxygen coordinations, octahedral and tetrahedral, or all in octahedral coordination with some oxygen vacancies is uncertain. In any case, we believe that both models of $Ba_2Tl_2O_5$ are related to the perovskite structure, especially when we consider the cation arrangement, and the $BaTlO_{2.5}$ blocks in the new phases are similar to those in the $Ba_2Tl_2O_5$ phase. The substitution of Tl for Ba in the perovskite-like $Ba_2Tl_2O_5$ phase demonstrates a new type of structure, but leaves open the question of oxygen content and atomic positions.

Recently in our laboratories, extra Bi cations have been successfully introduced into the Ba site in the $BaBiO_3$ material to form

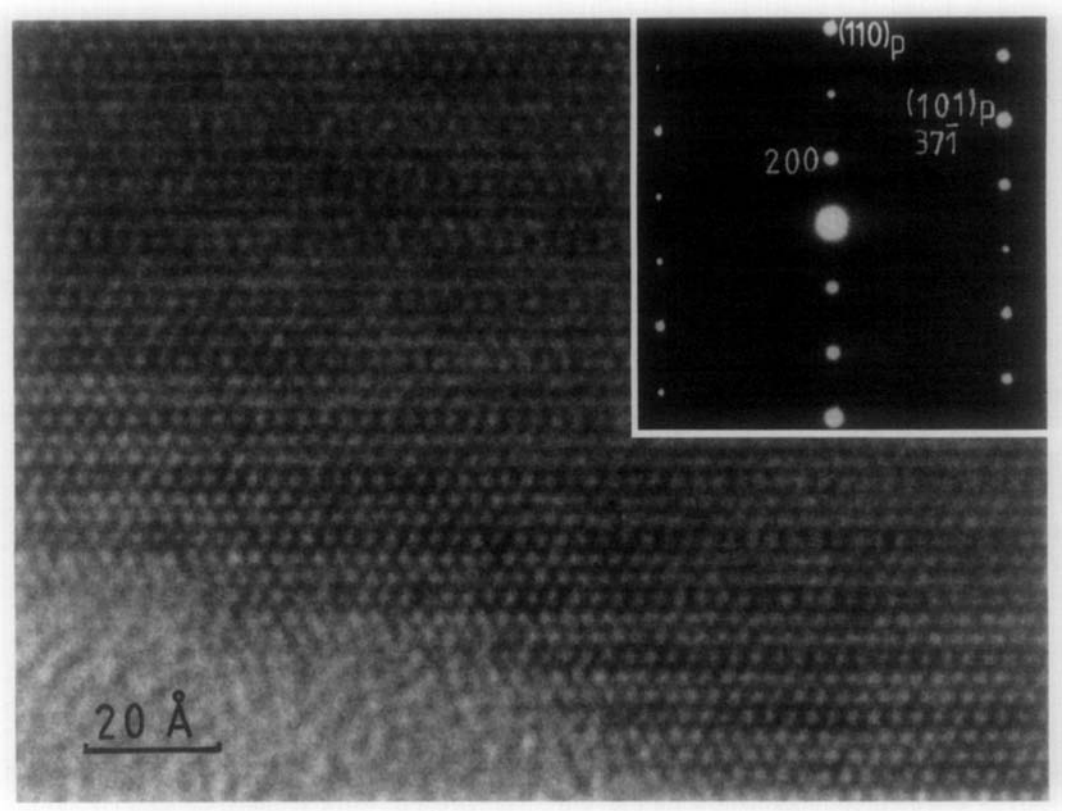

FIG. 5. High resolution electron microscopy images of $Ba_2Tl_{10}O_{17}$, viewed down the $[0\bar{1}\bar{7}]$ direction of the superstructure of the $[\bar{1}11]$ direction of the perovskite-like subunit cell. The inset is the corresponding SAED pattern indexed onto both the real unit cell by (hkl) and the perovskite subunit cell by $(hkl)_p$.

solid solution phases, $Ba_{1-x}Bi_{1+x}O_3$. When the amount of x is small, e.g., $Ba_{0.9}Bi_{1.1}O_3$, $Ba_{0.8}Bi_{1.2}O_3$, a lattice distortion was observed. In the composition of $Ba_{0.6}Bi_{1.4}O_3$, XRD showed a perovskite-like pseudocubic phase and HREM studies revealed a $4 \times 4 \times 4$ superstructure based on the perovskite subcell (*10*). Bearing in mind that to form a perovskite structure, ABO_3, the lattice tolerance factor $t = (R_A + R_O)/[\sqrt{2}(R_B + R_O)]$ must fall into a range of 0.8 to 1, where R is the ionic radii; the t value for $Ba^{2+}Bi^{5+}O_3$ is 0.91 and for $Ba^{2+}Bi^{3+}O_3$ is 0.82. Therefore, both Bi^{3+} and Bi^{5+} cations can fit the perovskite lattice with Ba^{2+} ions on the A sites, although we believe that all Bi cations in $BaBiO_3$ are equivalent according to our high resolution electron microscopy results (W. Zhou, *et al.*, unpublished work). On the other hand, the lattice tolerance factor for an imaginary compound, $Bi^{3+}Bi^{5+}O_3$, is 0.78, for $Bi^{+}Bi^{3+}O_3$, 0.71, and for $Bi^{+}Bi^{5+}O_3$, 0.79. The ionic radii of Ba^{2+} (1.34 Å), Bi^{+} (0.98 Å), Bi^{3+} (0.96 Å), Bi^{5+} (0.74 Å), and O^{2-} (1.32 Å) were used in the calculation. Bi cations occupying the Ba sites is unfavorable for the perovskite structure without oxygen vacancies when all the B sites are also occupied by Bi. Using the HREM technique, the detailed structures of the solid solution $Ba_{1-x}Bi_{1+x}O_3$ have been investigated. It is believed that the super-

structure is mainly due to an ordering of oxygen vacancies and most, if not all, of the Bi cations have a 3+ charge valence. Therefore, the oxygen content, y, in the $Ba_{1-x}Bi_{1+x}O_y$ should be less than 3. Oxygen vacancy might play an important role in stabilizing the structures.

Recently, Itoh *et al.* reported their successful synthesis and structural investigation of perovskite-related solid solution phases $Ba_{1+x}Bi_{1-x}O_y$ as well as $Ba_{1-x}Bi_{1+x}O_y$ (*11*). Oxygen vacancies seem to be common in these compounds and make it possible to exchange cations between the A and B sites in a perovskite lattice.

In the case of the Ba–Tl–O system, the perovskite lattice tolerance factor value for $Ba^{2+}Tl^{3+}O_3$ is 0.83. In fact, the oxygen content in this compound is 2.5 instead of 3 in an ideal perovskite structure and some Tl cations are no longer coordinated by six oxygens. Either Tl in tetrahedral coordination as reported previously (*5*) or in square pyramid coordination will certainly stabilize the lattice, since the whole lattice is compressed with less oxygen content. The lattice tolerance factor for $Tl^{+}Tl^{3+}O_3$ is 0.87, which seems to be acceptable for a perovskite structure. However, substitution of Ba^{2+} with Tl^{+} requires even less oxygen content. From the XRD and SAED patterns, the superlattices in the Ba–Tl–O compounds result from ordering of cations rather than ordering of oxygen vacancies. The existence of Tl^{+} is unlikely. Another possible model is $Tl^{3+}Tl^{3+}O_3$, in which Tl^{3+} cations occupy both A and B sites in a perovskite lattice and oxygen atoms shift from a perovskite lattice toward a pyrochlore-like lattice or even a fluorite-like lattice. Although fluorite, pyrochlore, and perovskite structures are quite different each other, slightly distorted forms of these structures can intergrow together in some solid solution materials, i.e., in the Bi–Nb–O system (*12*).

When the amount of substitution of Ba by Tl is small, the distortion of the perovskite basic lattice is significant. The more Tl substitution for Ba, the higher the lattice symmetry in the perovskite-like solid solution range as observed in $Ba_2Tl_{10}O_{17}$. This supports the conclusion that the superlattices are mainly due to ordered arrangements of the Ba and Tl cations.

The understanding of Tl diffusion from the *B* sites into the *A* site in a perovskite lattice is interesting when we examine the structure of the Tl-containing high Tc superconductors. In the $Tl_2Ba_2Ca_nCu_{n+1}O_{2n+5}$ compounds, the crystal structures are usually perfect without any detectable evidence of defects and superlattice. Therefore, all cations in these compounds were believed to be fully oxidized. Tl cations are 6-coordinated and Ba cations are 9-coordinated by oxygen ions. It is very possible that some Tl cations diffuse into the Ba sites: such a substitution would have a marked effect on the electronic properties of the materials.

The electrical resistivity measurements at room temperature show the ρ_{300K} value for $Ba_2Tl_2O_5$ is larger than 9×10^4, for $Ba_4Tl_6O_{13}$, 33.3, for $Ba_6Tl_{14}O_{27}$, 1.1×10^{-3}, and for $Ba_2Tl_{10}O_{17}$, 1.8×10^{-4} (Ω cm). The temperature dependence of the resistivity (suitably normalized to the respective values at room temperature) of the materials is shown in Fig. 6. Although we proposed that the structures of $Ba_4Tl_6O_{13}$, $Ba_6Tl_{14}O_{27}$, and $Ba_2Tl_{10}O_{17}$ are all related to perovskite, $Ba_4Tl_6O_{13}$ is a semiconductor, while the other two show metallic behavior. We believe that the lattice distortion plays a great role in determining this property. In addition, comparing the resistivities of these compounds with that of the C-type Tl_2O_3 (ca. 10^{-4} Ω cm at room temperature) (*1b*), the results support our argument that the structures of the series compositions in the BaO–Tl_2O_3 system transform from perovskite gradually toward fluorite when the Tl content increases from $Ba_2Tl_2O_5$ to $Ba_2Tl_{10}O_{17}$.

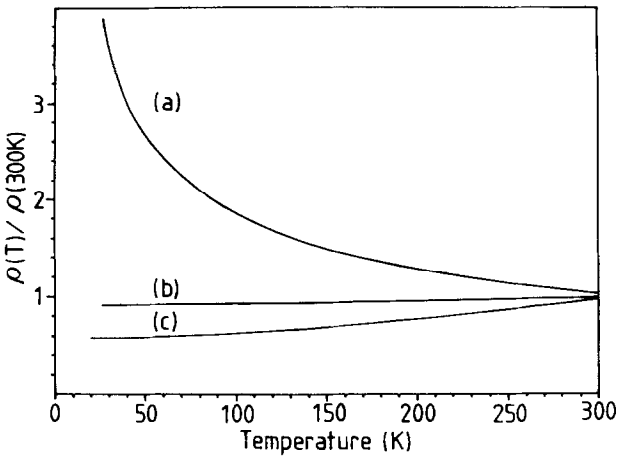

FIG. 6. Temperature dependence of the electrical resistivity measurements on (a) $Ba_4Tl_6O_{13}$, (b) $Ba_6Tl_{14}O_{27}$, and (c) $Ba_2Tl_{10}O_{17}$.

Consequently, although oxygen atomic coordinates are not fully understood in this present work, we report two new phases in the Ba–Tl–O system. These are superstructures derived from perovskite lattice with extra Tl cations entering the Ba sites. This information might be important in the field of superconducting oxides, since trace substitution of Ba by Bi or Tl could significantly effect the electronic properties of the materials.

Further investigations including the determination of oxygen content by chemical analysis, determination of oxygen positions possibly by neutron diffraction studies, and the measurement of physicochemical properties of these new materials are being carried out in these laboratories.

Acknowledgments

We express our thanks to SERC and B.P. for financial support and to Dr. D.A. Jefferson for helpful discussion.

References

1. (a) P. PAPAMENTELLOS, *Z. Kristallogr.* **126,** 143 (1967); (b) A. W. SLEIGHT, J. L. GILLSON, AND B. L. CHAMBERLAND, *Mater. Res. Bull.* **5,** 807 (1970).
2. W. ZHOU, D. A. JEFFERSON AND J. M. THOMAS, *Proc. R. Soc. Lond. A* **406,** 173 (1986).
3. W. ZHOU, *J. Solid State Chem.* **76,** 290 (1988).
4. W. ZHOU, R. S. LIU, R. JANES AND P. P. EDWARDS, *Mater. Lett.* **9**(4), 169 (1990).
5. A. COLVILLE, *Acta. Crystallogr.* **B26,** 1469 (1970).
6. VON R. V. SCHENCK AND HK. MULLER-BUSCHBANM, *Z. Anorg. Allg. Chem.* **405,** 197 (1974).
7. M. ITOH, R. LIANG, AND T. NAKAMURA, *J. Solid State Chem.* **82,** 172 (1989).
8. W. ZHOU, R. S. LIU, AND P. P. EDWARDS, *J. Solid State Chem.* **87,** 472 (1990).
9. D. A. JEFFERSON, J. M. THOMAS, G. R. MILLWARD, K. TSUNO, A. HARRIMAN AND R. D. BRYDSON, *Nature (London)* **323,** 428 (1986).
10. W. ZHOU, M. DALTON AND P. P. EDWARDS, manuscript in preparation.
11. M. ITOH, T. SAWADA, R. LIANG, H. KAWAJI, AND T. NAKAMURA, *J. Solid State Chem.* **87,** 245 (1990).
12. W. ZHOU, D. A. JEFFERSON, AND J. M. THOMAS, (a) *J. Solid State Chem.* **70,** 129 (1987); (b) Geophys. Monograph 45: "Perovskite: A Structure of Great Interest to Geophysics and Materials Science" (1989) 113.